Carbon structure in nanodiamonds elucidated from Raman spectroscopy

Vitaly I. Korepanov and Hiro-o Hamaguchi, National Chiao-Tung University, Taiwan
Eiji Osawa, NanoCarbon Research Ltd., Japan
Vladimir Ermolenkov and Igor K. Lednev, Department of Chemistry, University at Albany, SUNY, USA
Bastian J. M. Etzold, Lehrstuhl für Chemische Reaktionstechnik, Friedrich-Alexander-Universität Erlangen-Nürnberg, Germany
Olga Levinson and Boris Zousman, Ray Techniques Ltd, The Hebrew University of Jerusalem
Chandra Prakash Epperla and Prof. Huan-Cheng Chang, Institute of Atomic and Molecular Sciences, Academia Sinica, Taiwan

Contents

Abstract

Characterization of nanodiamonds (ND) is a difficult challenge due to the complex structure of nanoparticles: along with the diamond core it also contains graphene-like carbon (GLC), disordered carbon, significant number of lattice defects, and surface-state carbon, including polyacetylene chains and terminal groups. For the numerous applications of different types of nanodiamonds it is very important to characterize the content of various carbon fragments, as well as the size distribution of the diamond cores. In this work, we apply Raman spectroscopy to study the structure of nanodiamonds from different origins, including those produced by detonation (DND), high pressure high temperature synthesis (HPHT), and pulsed laser irradiation (LND). The relative content of GLC, disordered and surface carbon can be easily determined from Raman spectral patterns. In particular, we show how the content of different structure fragments is changed upon de-agglutination, surface oxidation and ion irradiation. We also compare the different ND fabrication methods in terms of the structural uniformity of the nanoparticles. Raman spectroscopy provides unique quantitative tool for ND characterization; we believe that the present data will be useful for understanding the structure of diamond nanoparticles, and will provide the background for obtaining the NDs with desired properties.

Keywords

Nanocarbon, Raman spectroscopy, Nanoparticles Structure, Phonon confinement, Particle size

Introduction

Diamonds nanoparticles represent a unique class of nanoscale systems with variable structure and tunable properties. At present, they can be obtained by several synthetic routes with different grain size ranging from sub-5 nm detonation nanodiamond (DND) to 10-1000 nm high-pressure-high-temperature (HPHT) nanodiamonds. Despite the commonly used name “nanodiamonds”, these nanoparticles are comprised of a complex interplay of different carbon phases. The structure can be perceived as more or less crystalline diamond core surrounded by the shell, consisting of graphene-like carbon (GLC) and disordered sp3 carbon. In addition, the surface is usually grafted by oxygen-containing groups (-OH, >C=O), unless it is hydrogenated by hydrogen plasma treatment. Some portion of the shell is the by-product of the ND synthesis and can be eliminated, for example, by oxidation or plasma etching. However, there are also intrinsic components of the shell, coming from the re-arrangement of the diamond surface. They include GLC islets and fullerene-like fragments on the surface of the core [1]. With the decrease of the particle size, the shell plays increasingly important role in physical and chemical properties of the material.

The wide range of the particle sizes, and easily achievable variety of surface terminations result in numerous applications of NDs in biomedicine, material technology, abrasives, lubricants, imaging, and many other fields [2]. The fast and reliable characterization of different carbon phases and their changes upon different physical and chemical treatments is of major importance for the ND-related research and technology. In the present work we address this problem by Raman spectroscopy. We analyze the dependence of the diamond Raman band on the crystallite size, and study how the content of different structural fragments is influenced by the common techniques of ND processing, including de-agglutination, surface oxidation and nitrogen ion irradiation.

Raman spectral pattern and assignment of the bands

The complexity of ND structure is revealed in the Raman pattern as a superposition of bands coming from the nanocarbon fragments of different bonding [3,4]. The Raman cross-sections for different nanocarbon types also depend on the excitation wavelength in different ways [3]. On the other side, the bands coming from different structure fragments can be easily identified and distinguished, which makes it possible to characterize the relative content of those in the material.

The assignment of the spectral features of different nanocarbons is by now well established; the reader can refer to the works [3,4] and references therein for more details. We summarize the spectral assignment in fig. 1, with the spectra measured at three different excitation wavelengths for the same sample.

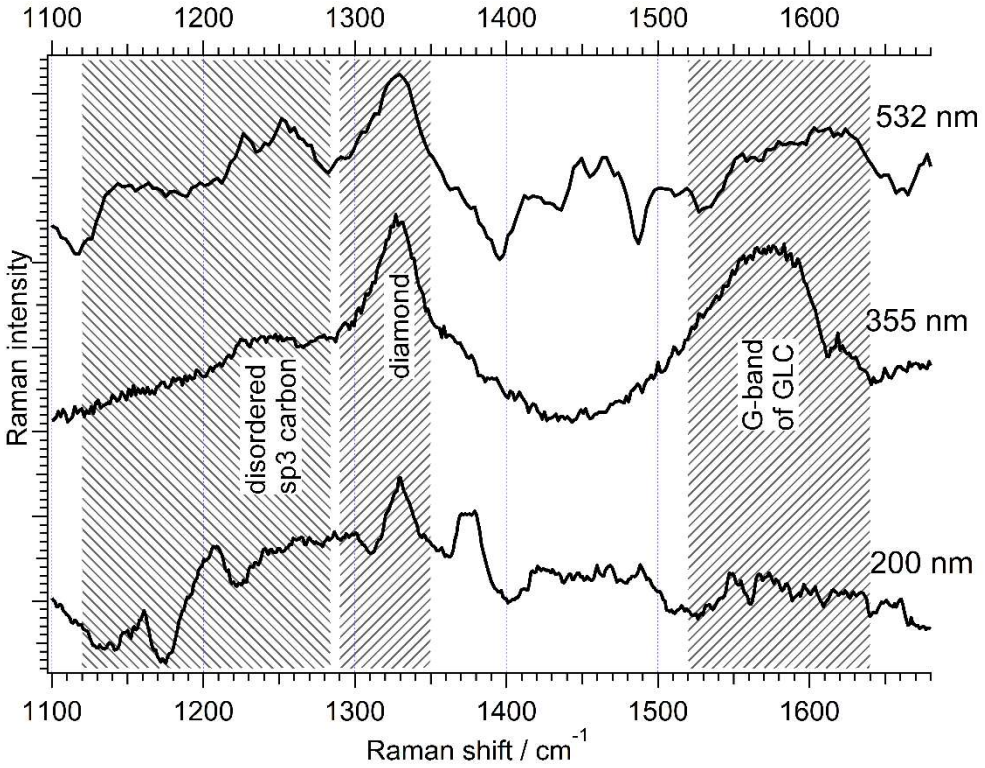

Figure 1. Experimental Raman spectra of 3 nm DND at different excitation wavelengths; the major bands of different types of nanocarbon highlighted.

The major bands in the Raman spectra of NDs are:

1) The diamond band for the bulk crystal is observed as a sharp line at around 1333 cm^{-1}; for ND it gives a broad peak in 1290-1350 cm^{-1} region, the position and width depends on the crystallite size [5].

2) Graphene-like carbon gives the G and D peaks, which lie at ~1560 and 1360 cm^{-1} respectively [3]. The G peak position shows dispersion (excitation wavelength dependence) [3]. In our experiments, the D peak is most pronounced at 200 nm excitation, while in the 355 and 532 nm spectra it appears as a shoulder.

3) Disordered sp3 carbon gives a broad feature in 1100-1350 cm-1, the shape of which corresponds to the density of states (DOS) [4].

4) Trans-poly-acetylene carbon on the surface gives a peak at around 1150 cm^{-1} [4].

5) the dumbbell, aka split-interstitial defect of diamond lattice, shows a relatively sharp band at 1630 cm^{-1} [4].

In the present work, we aimed to study the structure of nanodiamonds of different origins, and examine the impact of various treatment procedures on the structure. As can be seen from fig. 1, most convenient for this purpose is to use the distinct bands of diamond, disordered sp3 carbon and G-band of GLC measured at 355 nm excitation, because the contribution from non-carbon bands is relatively low, and the bands from different carbon fragments can be easily distinguished from each other.

Experimental detection of the ND Raman spectra

The main difficulty of the experimental detection of ND Raman spectra is that the sample is typically the black powder, which absorbs the light throughout the whole UV-Vis spectral range. Therefore, under the laser beam the sample can be easily heated or burned out. To overcome this problem, different groups either use low laser power or try to measure under water [6]. From our experience, the use of rotating cell with the ND sample dispersed in water allows one to obtain high signal-to-noise ratio spectra without the need to reduce the laser power [5]. In addition to that, this technique helps to avoid the thermal distortion of the phonon spectrum, and provides a good averaging over the sample.

Another challenge is to achieve good signal-to-noise ratio. Most of ND samples give quite strong luminescence, coming, most likely, from GLC fragments on the surface. The luminescence dominates the spectrum at 632 nm excitation to an extent that practically no Raman band is observable for most of the samples. With decreasing excitation wavelength the Raman-to-luminescence ratio becomes higher. Under deep UV (200 nm) practically no luminescence is observed. On the other hand, in deep UV spectra many Raman bands from surface groups and defects become quite strong (see fig. 1), and the carbon bands are difficult to analyze. The reasonable balance from our experience is to use UV excitation at 355 nm, under which the luminescence background can be easily subtracted, and the Raman bands of different carbon fragments can be distinguished.

From our observation, the Raman-to-luminescence ratio can also be significantly improved by the oxidation of the surface carbon (e.g. 425°C in air), therefore for some measurements the samples can be pre-treated to get better spectra.

“Raman size” of nanodiamonds

The crystallite size estimation is of major importance for the numerous applications of nanodiamond. The common techniques used for that purpose include transmission electron microscopy (TEM), dynamic light scattering (DLS), X-ray diffraction and small-angle X-ray diffraction (SAXS). It must be understood that these methods by their nature are supposed to estimate different physical parameters. TEM can give the image of the particles at the focal plane, and, therefore, give a rough estimate of the particle size and the crystallite size for a very limited portion of the sample. The DLS measures hydrodynamic radius, which includes surface layers and detects aggregates as a single particle. X-ray diffraction used with the Scherrer equation possesses certain degree of arbitrariness, although for high signal-to-noise ratio diffraction patterns the size distribution of crystallites still can be roughly estimated [7]. The disadvantage of XRD is the low sensitivity to the size. The SAXS is a reliable and sensitive method for estimating the grain size of nanopowders [8]. The grain size although does not coincide with the diamond core size, because SAXS does not make distinction between different types of carbon.

The "Raman size" for crystalline materials can be defined as the phonon confinement length, or, in other words, the size of coherently scattering domain. In case of diamond it corresponds to the crystallite size of the diamond core, because Raman spectroscopy can distinguish the diamond lattice band from the other structural fragments. Other advantages of Raman spectroscopy are relatively high size sensitivity, statistical reliability and comparatively simple experimental measurement.

The established approach linking the Raman band shape to the phonon confinement length, known as Phonon Confinement Model (PCM) was proposed by Richter [9]. Applying it to diamond, many research groups used simplified one-dimensional description of the phonon dispersion, which introduces certain degree of arbitrariness. We have recently reported the physically consistent way of building the PCM, which includes not only 3D phonon dispersion, but also size distribution and other minor improvements. Hereafter, we will use the working formula from the work [5]:

$$I(\omega) \cong \int \rho(\sigma) d\sigma \frac{\sigma^3}{N(\sigma)} \iiint \frac{\Gamma_0(\sigma) * \left|C(q_0,q)^2\right|^2}{\left(\omega - \omega(q)\right)^2 + \left(\Gamma_0(\sigma)/2\right)^2} d^3q \qquad (1)$$

where □ is the wavenumber, □(□) is the particle size distribution, $N(\sigma)$ is the normalizing factor, $C(q_0,q)$ is the Fourier coefficient, □(q) is the three-dimensional (3D) phonon dispersion function, □₀ is the natural bandwidth. As has been shown before [5], the good description of the dispersion function can be obtained using scaled quantum-chemical frequencies. The PCM has proved to adequately account for the size dependence of the Raman spectra of nanodiamonds. The simulated spectral patterns of monodisperse NDs of different size are shown in fig. 2.

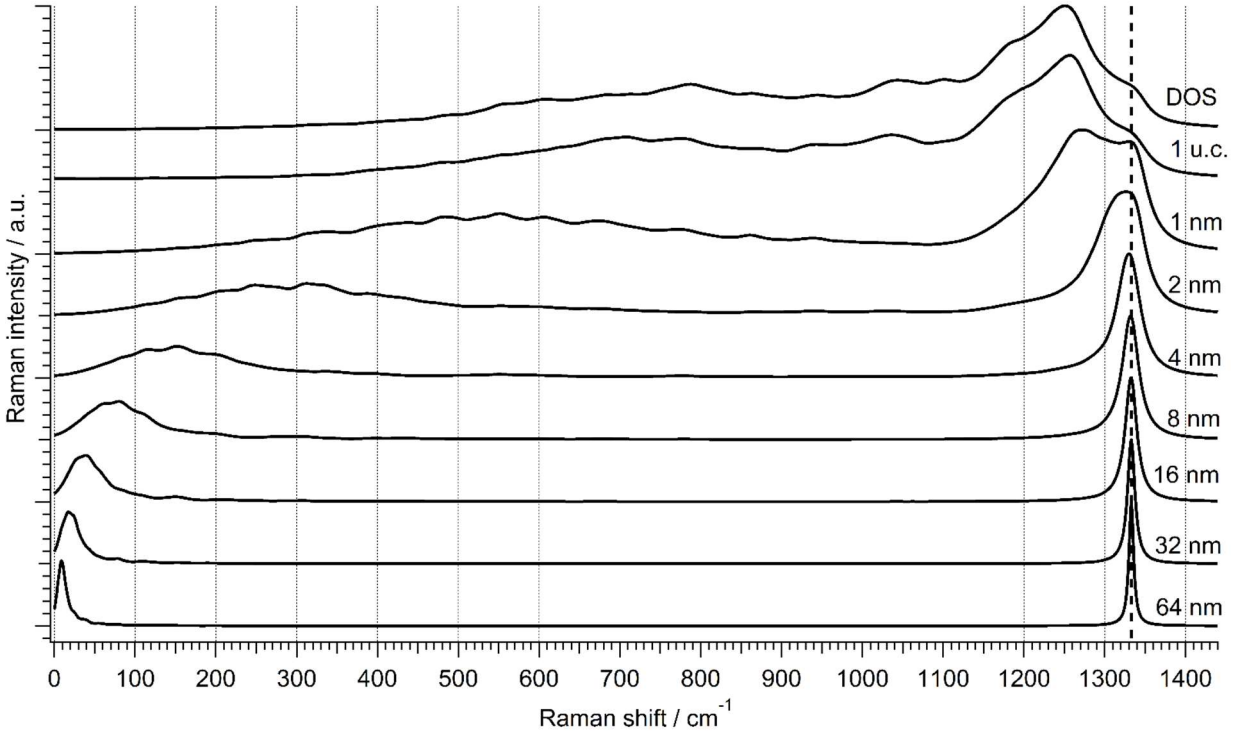

Figure 2. Hypothetical calculated Raman spectra for different confinement lengths starting with disordered sp3 carbon network (DOS), next is 1 unit cell (1 u.c.) confinement (i.e. 0.3567 nm). The vertical line indicates the frequency at the Γ point (1332.9 cm^{-1}).

Materials and methods

ND samples and procedures of physical and chemical treatment

- DND3, de-agglutinated detonation nanodiamond colloid, with mean size of 3.3 nm (as estimated from DLS), NanoCarbon research Institute Ltd., Japan.
- DND3 irradiated with nitrogen ions. Experimental set-up was provided as a courtesy of Nagata Seiki, Japan. 20 keV nitrogen beam was used. The nitrogen pressure at the plasma generator was $3.5*10^{-2}$ Pa; the current was 20 μA. The sample load was 300 mg. Irradiation was performed 2 times during 40 minutes. In between the two irradiations the sample was carefully mixed.
- DND agglutinates, the raw material used for the production of DND3.
- DND3 oxidized, the DND3 sample after oxidation in air at 420°C within 20hr.
- DND LbL0, the ND from Adamas Nanotechnologies Inc.
- DND LbL15, the NDN LbL0 sample after 15 cycles of Layer-by-Layer oxidation [8].
- LND, laser-synthesized ND with 4 nm mean size (as estimated by XRD), Ray Techniques Ltd., Israel;
- 23nm HPHT, high-pressure high-temperature diamond, acid-washed and air-oxidized (3-4 hr at 450°C), with mean size 23 nm (as estimated by DLS), Institute of Atomic and Molecular Sciences, Academia Sinica, Taiwan.
- 29 HPHT diamond, treated in the same way, with mean size 29 nm,
- 42 HPHT diamond, treated in the same way, with mean size 42 nm.

Spectral measurements

The Raman spectra were measured with lab-built confocal systems under 632 nm, 532 nm, 355 nm and 200 nm excitation wavelengths. The samples were in the form of the 1% ND colloid in water. The colloids were ultrasonicated in a horn during at least 0.5 hr prior to the measurement. To avoid the effects of laser heating, the rotating quartz cell was used.

Computational procedures

The PCM fitting of the diamond band was performed with the help of Matlab and Quantum Espresso [10] software as described elsewhere [5].

Results and discussions

The Raman spectra of the major ND samples are shown on fig. 3. For the bulk diamond spectrum has only one sharp symmetric line, while for NDs the diamond line is asymmetrically broadened, and in addition to that the GLC band and amorphous sp3 bands are observed. The diamond band shows pronounced dependence on the crystallite size.

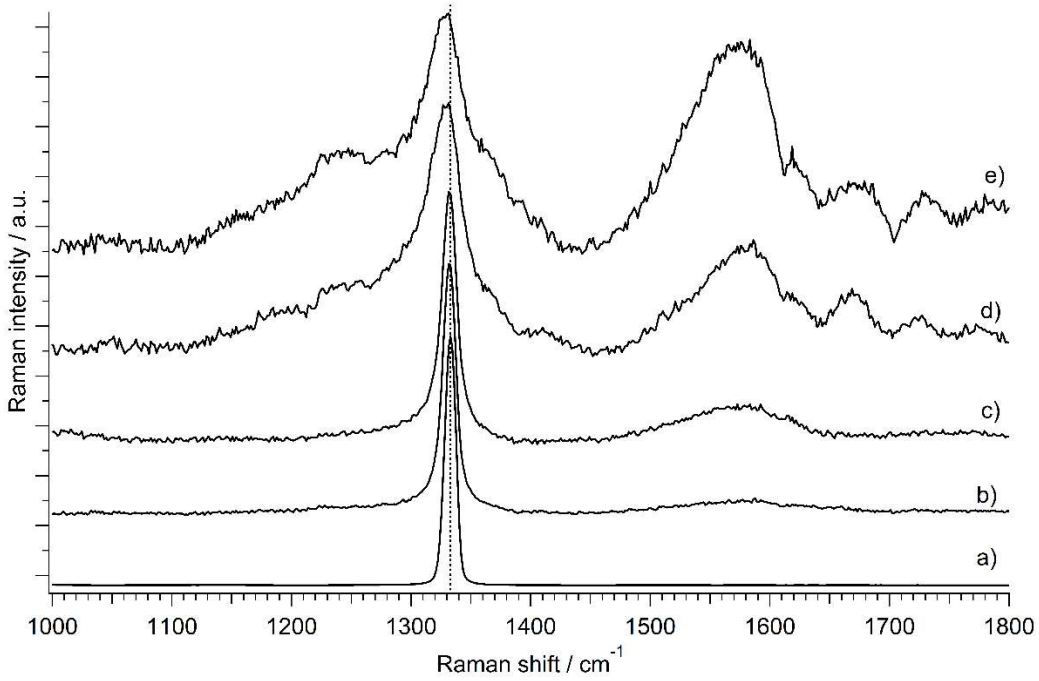

Figure 3. Representative ND samples of different mean size and origin: 35μm CVD microcrystal (a), 42nm HPHT (b), 23nm HPHT (c), 4nm LND (d) and 3nm DND (e). The position of the zone-center phonon (1332.9 cm^{-1}) is indicated by the dotted line.

In the present work, the diamond line was interpreted with the PCM (eq.1) to estimate the crystallite size. After that, the diamond line was subtracted and the ratios (area intensities) of the diamond line, G-band of GLC and the amorphous diamond band were estimated. This procedure is illustrated in fig. 4. The results are summarized in table 1.

Table 1. Quantitative analysis of the Raman spectra of different nanodiamond samples.

Sample*	**median size estimated from PCM**	**median size by other estimations**	**diamond to amorphous ratio**	**diamond to GLC ratio**
de-agglutinated DND (DND3)	2.9	3.3 (DLS)	1.02	0.55
DND3 irradiated with N_2^+	2.2	---	0.71	0.32
DND3 oxidized in air	2.9	2.7 (DLS)	1.41	1.17
raw DND agglutinates	2.9	---	0.89	0.82
DND LbL 0	3.0	5.2 (SAXS)	0.88	0.86
DND LbL 15	3.0	4.8 (SAXS)	1.42	1.05
laser-synthesized ND (LND)	3.5	4.0 (XRD)	1.27	1.12
23nm HPHT ND (ox)	21.6	23 (DLS)	2.30	1.24
29nm HPHT ND (ox)	28.8	29 (DLS)	3.16	2.52
42nm HPHT ND (ox)	42.4	42 (DLS)	2.51	2.46

* see materials and methods section for more details about the history of the samples

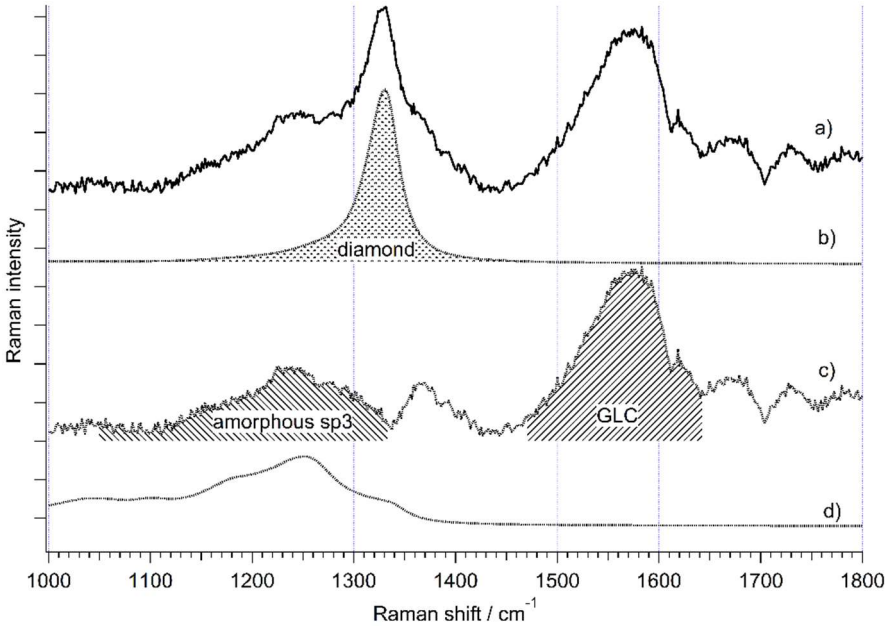

Fig. 4. The procedure of analyzing the ND spectra: the experimental spectrum (a), fit of the diamond band with PCM equation (b), ND spectrum after subtraction of the diamond band (c), DOS of diamond shown to confirm assignment of the amorphous diamond band (d).

This quantification procedure allows us to compare the different ND production method, as well as to analyze how the structure of ND particles is influenced by the common techniques of ND processing, such as de-agglutination, surface oxidation and ion irradiation.

a. de-agglutination

The process of preparation of well-dispersed ND colloid, also known as de-agglutination, includes beads milling and ultrasonication [11]. During the beads milling, the local pressure and temperature can be high enough to have impact on the nanoparticle structure. By means of Raman spectroscopy we can study what was the change.

As can be seen from table 1, the diamond-to-amorphous carbon ratio is increased upon de-agglutination, while the diamond-to-GLC ratio is slightly decreased. The difference in the spectra between raw and de-agglutinated samples is shown in fig. 5. Thus, the local pressure and temperature induce moderate graphitization, most likely graphitized might be the amorphous sp3 carbon from the ND shell. The crystallite size of the ND doesn't show detectable difference which indicates that the diamond core remains practically the same.

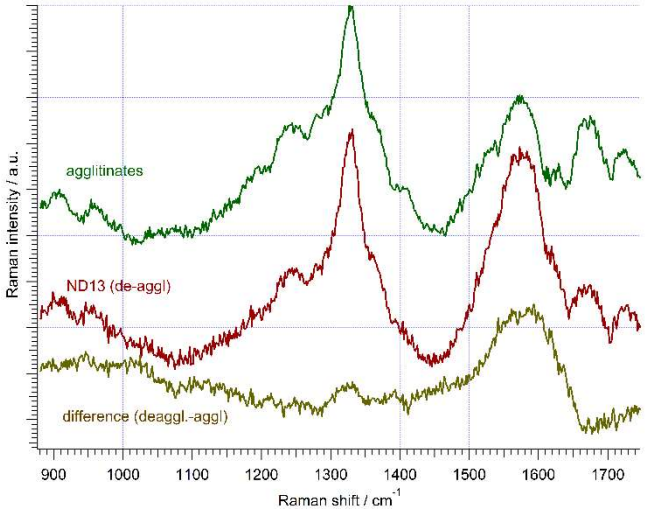

Figure 5. Raman spectra of raw DND agglutinates (top), de-agglutinated sample (middle) and the difference (bottom).

b. surface oxidation

The controlled oxidation of nanodiamonds is expected to reduce the particle size. On the other hand, since smaller particles are expected to burn out more quickly, the average particle size may also increase. It is also reasonable to expect that defective carbon would oxidize more easily than highly ordered. We studied by Raman spectroscopy the ND samples after two different modes of oxidation: by air and layer-by-layer (LbL). In contrast to air oxidation, the LbL etching allows one to avoid a runaway oxidation reaction of small particles [8]. The oxidation in air was performed at relatively soft temperature of 425°C during 20 hours (mean DLS size reduced from 3.3 to 2.7 nm); the LbL etching was done within 15 sorption-desorption cycles (the SAXS size reduced from 5.2 to 4.8 nm).

The spectra of oxidized NDs are compared to those of starting samples in Fig. 6. It can be seen that in both oxidation regimes the difference spectrum has major contribution from D and G peaks of GLC along with amorphous carbon bands. The peaks on the both sides of diamond band (1270-1370 cm^{-1}) can also belong to very small crystallites (below 1 nm), see fig. 2.

The surprising finding is that the raw and oxidized spectra have almost identical diamond band, which is hardly distinguishable by PCM. From the point of view of ND structure it means that the surface is covered by GLC and amorphous carbon, which is etched in both oxidation modes, while the diamond core remains practically unchanged. Therefore, the particle size decrease detected by SAXS in LbL etching and DLS in air oxidation can be assigned mostly to the etching of non-diamond carbon from the nanoparticle shell.

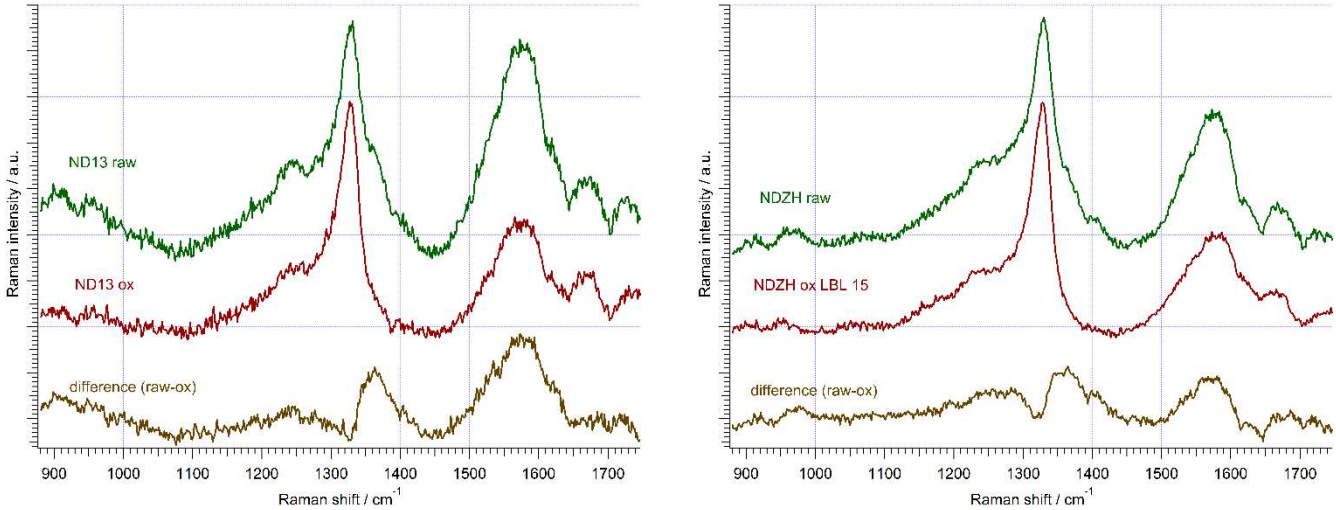

Figure 6. Oxidation of ND by air (left) and layer-by-layer etching (right). Top curves: spectra of original samples, middle: oxidized, bottom: difference.

c. nitrogen ion irradiation

Ion irradiation, typically used to introduce defects in diamond lattice, has quite strong impact on the ND structure. As can be seen from table 1 and fig. 7, after the irradiation the G-band of GLC becomes almost twice stronger, the pronounced increase of amorphous sp3 carbon band is also observed. The diamond crystallite size determination by PCM is less reliable in case of irradiated

sample, because the diamond peak is strongly superimposed by other bands. However, the PCM results in this case show quite expected decrease of phonon confinement length, which can be attributed most likely to the confinement by the lattice defects.

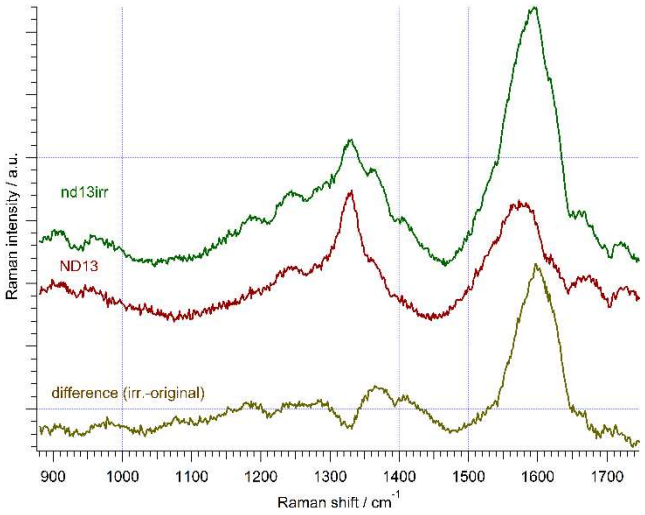

Figure 7. The effect of nitrogen ions irradiation on the ND structure: Raman spectra of irradiated sample (top), original sample (middle), and the difference (bottom).

d. comparison of ND production methods

The main quantitative criteria to compare the production methods of NDs are the peak ratios of diamond to GLC and diamond to amorphous sp3 carbon. From table 1 it can be seen that the raw DND agglutinates both from NCRI and Adamas Nanotechnologies (DND LbL 0) have lower content of diamond than LND. The raw HPHT diamonds have very high GLC content, which didn't allow us to measure the Raman spectra of un-oxidized samples. For the oxidized ones, the diamond content is relatively high, but taking into account the much higher particle size, the GLC content is still very significant. Therefore, among the studied samples, the most structurally uniform diamond nanoparticles seem to be produced by the laser irradiation. The structural uniformity of NDs can be significantly improved by the surface oxidation.

Conclusions

Raman pattern of nanodiamonds contains important information on the structure of nanoparticles, such as crystallite size and the content of GLC and amorphous sp3 carbon. This allows us to study the behavior of different structure fragments during chemical and physical treatment. Diamond nanoparticles consist of the inert and stable diamond core, surrounded by the shell of amorphous sp3 carbon and GLC, which more easily undergoes transformations. Thus, de-agglutination procedure is accompanied by minor graphitization of the shell due to local heat/pressure effect. Oxidation treatment in both layer-by-layer and air-oxidation regimes results in the decrease of GLC and amorphous carbon content, while the diamond core remains practically the same. The irradiation of NDs with nitrogen ions results in both decrease of the crystallite size and pronounced graphitization.

Quantitative study of the Raman spectra of different NDs makes possible to compare different ND production methods in terms of the structural uniformity of the resulting material. Among the studied samples (DND, LND, HPHT-ND) the laser-assisted synthesis gives the most pure "diamond"

material with lowest content of GLC and amorphous carbon. The structural uniformity of NDs can be significantly improved by the surface oxidation under mild conditions.

Raman spectroscopy is an important quantitative tool to analyze the ND spectra, and we believe the present results would assist the synthesis of the NDs with desired properties and assist the development of the nanocarbon technology.

Acknowledgment

This work was supported by EU Horizon 2020 MSCA-RISE grant (Project 690945 "Carbon-based nano-materials for theranostic application") which is gratefully acknowledged.

References

[1] Y. V. Novakovskaya and A. V. Vorontsov, Struct. Chem. **26**, 1297 (2015).
[2] V. N. Mochalin, O. Shenderova, D. Ho, and Y. Gogotsi, Nat. Nanotechnol. **7**, 11 (2011).
[3] A. C. Ferrari and J. Robertson, Philos. Trans. A. Math. Phys. Eng. Sci. ***362***, 2477 (2004).
[4] S. Prawer, K. W. Nugent, D. N. Jamieson, J. O. Orwa, L. A. Bursill, and J. L. Peng, Chem. Phys. Lett. ***332***, 93 (2000).
[5] V. I. Korepanov and H. Hamaguchi, Arxiv Prepr. 6 (2016).
[6] S. Osswald, V. Mochalin, M. Havel, G. Yushin, and Y. Gogotsi, Phys. Rev. B **80**, 75419 (2009).
[7] R. Pielaszek, J. Alloys Compd. ***382***, 128 (2004).
[8] B. J. M. Etzold, I. Neitzel, M. Kett, F. Strobl, V. N. Mochalin, and Y. Gogotsi, Chem. Mater. **26**, 3479 (2014).
[9] H. Richter, Z. P. Wang, and L. Ley, Solid State Commun. ***39***, 625 (1981).
[10] P. Giannozzi, S. Baroni, N. Bonini, M. Calandra, R. Car, C. Cavazzoni, D. Ceresoli, G. L. Chiarotti, M. Cococcioni, I. Dabo, A. Dal Corso, S. de Gironcoli, S. Fabris, G. Fratesi, R. Gebauer, U. Gerstmann, C. Gougoussis, A. Kokalj, M. Lazzeri, L. Martin-Samos, N. Marzari, F. Mauri, R. Mazzarello, S. Paolini, A. Pasquarello, L. Paulatto, C. Sbraccia, S. Scandolo, G. Sclauzero, A. P. Seitsonen, A. Smogunov, P. Umari, and R. M. Wentzcovitch, J. Phys. Condens. Matter **21**, 395502 (2009).
[11] M. Ozawa, M. Inaguma, M. Takahashi, F. Kataoka, A. Krüger, and E. Ōsawa, Adv. Mater. **19**, 1201 (2007).